Mosquito Systematics, 25(2):124–147, 1993

A DESCRIPTION AND MORPHOMETRIC STUDY OF THE EGGS OF SPECIES OF THE *ANOPHELES QUADRIMACULATUS* COMPLEX (DIPTERA: CULICIDAE)

JOHN R. LINLEY[1], PAUL E. KAISER[2] AND ANDREW F. COCKBURN[2]

ABSTRACT. Descriptions and a morphometric analysis, based on scanning electron micrographs, are given of the eggs of the five known species of the *Anopheles quadrimaculatus* complex. Following an initial account of the fine structure of the eggs, represented by species A, electron micrographs are used to illustrate interspecific differences visible at low magnification in whole eggs and at higher magnification as appropriate for particular structural features. Extensive tabulations and synoptic comparisons are given of 42 attributes of the eggs. For multivariate analysis, 13 characters were selected and used as the basis for principal component and discriminant function analyses. The first seven principal components accounted for 91.18% of the variation, while the first two discriminant functions captured 90.97% of differences between species. Classification by discriminant functions of 87 eggs examined was successful in assigning 85 correctly to species. The study suggests that species C1 and C2 are the most closely related in the complex and are followed in relatedness by species A and B; species D is closer to C1 and C2 than to A and B.

INTRODUCTION

Anopheles quadrimaculatus (Say) was the primary vector of malaria and remains the most widely distributed and important anopheline in the eastern United States. Until recently, *An. quadrimaculatus* was considered to be a single species, but a complex of at least five separate species is now recognized. Species A and B were first described from populations in the southeastern United States (Lanzaro 1986, Kaiser et al. 1988a, Lanzaro et al. 1988, Narang and Seawright 1988), species C was discovered in west Florida (Kaiser et al. 1988b), and collections from Mississippi and west Florida revealed species D (Narang et al. 1989b). Narang et al. (1990) observed allelic differences among allozymes of coastal populations of species C, which justified a tentative division into C1 and C2. Formal evidence of this division remains to be published (Kaiser, unpublished data); however, in this paper we refer to them as two separate species, C1 and C2.

There are no obvious morphological characters that distinguish adults of the *An. quadrimaculatus* complex, although comparative taxonomic studies have never been done. Instead, their diagnoses and relationships have been studied entirely by cross-mating, polytene chromosome analysis, starch gel electrophoresis, and molecular genetic methods (Narang and Seawright 1991, Mitchell et al. 1992). To broaden the approach to include morphology, we considered it worthwhile to undertake an ultrastructural study of the eggs, because material of all five species could be collected with relative ease. The study offered three potentially important contributions: (1) confirmation or modification of the understanding of species relationships gained from genetic and cytological studies, (2) provision of detailed descriptions of the eggs of the five species, and (3) evaluation of the usefulness of egg morphology in understanding anopheline species complexes. Accordingly, we first provide a formal description of the detailed morphological features of the egg (based on species A), followed by a general comparison

[1] Florida Medical Entomology Laboratory, IFAS, University of Florida, 200 9th St. S.E., Vero Beach, FL 32962.
[2] USDA, ARS, Medical and Veterinary Entomology Research Laboratory, P.O. Box 14565, Gainesville, FL 32604.

of the species and a more detailed morphometric analysis.

MATERIALS AND METHODS

Source of material, confirmation of identity, fixation. Eggs were examined from six females of species A, B, C1, and C2 and five species of D, collected from daytime resting sites in the following localities.

Species A—Ogeechee River, Effingham Co., GA (3♀); Orlando colony, Gainesville, FL (3♀)
Species B—Ogeechee River, Screven County, GA (3♀); Manatee Springs State Park, Levy Co., FL (3♀)
Species C1—Bear Bay Swamp, Dixie Co., FL
Species C2—Choctawhatchee River, Walton Co., FL
Species D—Choctawhatchee River, Walton Co., FL

The gravid, field-collected (except species A, Orlando colony) females were induced to lay eggs in vials containing wet filter paper and a small amount of water. Once they had oviposited, the females were frozen and held for starch gel electrophoresis to determine species (Narang et al. 1989a, 1989b, 1990), while the eggs were allowed to embryonate for 24 hr before being fixed in alcoholic Bouin's solution.

Preparation for scanning electron microscopy. Fixed eggs were washed in two changes of 80% ethanol to remove picric acid and were dehydrated completely to 100% ethanol by 5% concentration increments. They were then dried by the critical point method, positioned on stubs previously covered with sticky tape, sputter-coated with gold, and examined immediately in a Hitachi S-510 scanning electron microscope. Eggs of only one species were processed and examined at a time because the eggs collapsed and buckled within 24 hr.

Eggs examined, micrographs recorded, data acquisition and analysis. Measurements and counts were made from three eggs from each female of each species (Table 1). Thus, 18 eggs were examined for species A, B, C1, and C2, 15 for species D. Most measurements came from a ventral view (200×) of the whole egg or from a micrograph (4,000×) of the tubercles in the central area of the anterior deck. Additional attributes were measured from supplemental micrographs of other eggs of the same females (Table 2) as follows: cell and pore areas in the ventral and dorsal plastrons from one micrograph (1,000×, each surface) of an area approximately in the middle of the egg; lobed tubercle characters from a micrograph (2,000×) of the anterior group of lobed tubercles; micropyle data from a micrograph (2,000×) of the micropyle of each of two eggs per female. All linear and area measurements were done with a digitizing tablet and SigmaScan software (Jandel Scientific, San Rafael, CA), and statistical analysis was performed with Statgraphics software (Statistical Graphics Corporation, Rockville, MD). When the anterior and posterior decks were connected, areas were measured after a dividing line had been drawn at half the egg length. Measurement of the area of the ventral plastron required a specific criterion for deciding its boundaries at the anterior and posterior ends of each float, where it was continuous with the plastron on the lateral surface (Fig. 1). Demarcation lines, beginning at the approximate positions at which the float margins began to curve sharply toward the dorsal surface, were drawn (following individual cell boundaries) on a slight diagonal to the deck margin, and the ventral area delimited was digitized (summation of two areas was required for some eggs, e.g., species A and B). In referring to dimensions of the chorionic cells, length is in the longitudinal axis of the egg; width is the circumferential dimension. Means cited in the text are given ± SE and were derived from an equal number of measurements from each egg of the particular species.

Definitions of attributes, terminology. In all, 42 attributes of the eggs were measured, counted, or calculated (percentages, ratios), 27 associated with the ventral views of whole eggs or the anterior deck tubercles (Table 1) and 15 from supplemental micrographs (Ta-

Table 1. Attributes[1] of eggs of the five species of *An. quadrimaculatus* measured from three eggs from each of six females (species A, B, C1, C2) or five females (species D).

Attribute	Mean (± SE)[2] for species				
	A (n = 18)	B (n = 18)	C1 (n = 18)	C2 (n = 18)	D (n = 15)
Linear dimensions[3]					
Egglen	551.4 ± 8.1b	529.7 ± 8.1ab	541.6 ± 8.2b	512.9 ± 4.4a	547.9 ± 4.4b
Eggwid	192.9 ± 2.5a	192.6 ± 5.6a	189.9 ± 1.9a	181.9 ± 1.5a	193.4 ± 2.9a
Lenwidrat	2.86 ± 0.02a	2.83 ± 0.04a	2.85 ± 0.03a	2.82 ± 0.03a	2.84 ± 0.04a
Float attributes					
Mnfltlen	285.6 ± 4.5bc	253.1 ± 5.2a	286.3 ± 5.1c	267.9 ± 3.6ab	273.4 ± 4.9bc
Fltpcn	51.8 ± 0.4bc	47.8 ± 0.4a	52.9 ± 0.6c	52.2 ± 0.4bc	50.3 ± 0.6b
Mnribs	23.1 ± 0.4b	20.7 ± 0.4a	21.1 ± 0.3a	20.4 ± 0.3a	20.7 ± 0.5a
Fltlenprib	12.4 ± 0.2ab	12.3 ± 0.2a	13.6 ± 0.1c	13.2 ± 0.2bc	13.3 ± 0.3c
Deck dimensions[4]					
Arwhlegg	739.10 ± 18.09b	679.63 ± 12.06a	760.67 ± 15.04b	653.94 ± 8.68a	748.67 ± 12.77b
Arantdk	212.19 ± 7.76c	207.77 ± 8.24c	141.36 ± 4.50b	118.31 ± 4.27ab	103.45 ± 8.01a
Arposdk	181.09 ± 6.46c	159.78 ± 8.86c	128.41 ± 5.48b	104.88 ± 4.36ab	85.02 ± 4.25a
Artotdk	393.28 ± 13.86c	367.56 ± 16.01c	269.78 ± 9.46b	223.20 ± 7.67a	188.48 ± 10.32a
Antdkpcn	28.6 ± 0.4c	30.4 ± 0.8c	18.6 ± 0.5b	18.1 ± 0.6b	13.8 ± 0.9a
Posdkpcn	24.5 ± 0.4c	23.4 ± 1.2c	16.9 ± 0.6b	16.1 ± 0.6b	11.3 ± 0.5a
Totdkpcn	53.0 ± 0.7c	53.8 ± 1.9c	35.5 ± 1.1b	34.2 ± 1.1b	25.1 ± 1.2a
Dkrat	1.17 ± 0.02ab	1.35 ± 0.06b	1.11 ± 0.03a	1.14 ± 0.04a	1.24 ± 0.09ab
Antdklenwidrat	2.41 ± 0.04c	2.28 ± 0.05bc	1.99 ± 0.05a	2.02 ± 0.06ab	2.31 ± 0.12c
Posdklenwidrat	2.79 ± 0.05c	2.83 ± 0.07c	2.17 ± 0.06ab	2.08 ± 0.11a	2.44 ± 0.11b

Table 1 continues.

Table 1. *Continued.*

Attribute	Mean (± SE)[2] for species				
	A (n = 18)	B (n = 18)	C1 (n = 18)	C2 (n = 18)	D (n = 15)
Ventral plastron					
Arvnplas	62.44 ± 2.18a	47.42 ± 6.88a	167.62 ± 10.49c	115.05 ± 6.67b	177.15 ± 6.58c
Vnplaspcn	8.5 ± 0.4a	7.2 ± 1.1a	21.9 ± 1.1c	17.6 ± 0.9b	23.9 ± 1.1c
Noplascel	34.8 ± 1.1a	28.0 ± 2.1a	66.6 ± 3.8c	54.1 ± 3.4b	77.9 ± 2.9c
Lobed tubercles					
Noantlobtb	6.6 ± 0.2b	5.2 ± 0.3a	8.6 ± 0.3c	6.6 ± 0.3b	6.8 ± 0.3b
Noposlobtb	7.3 ± 0.3b	5.1 ± 0.3a	7.7 ± 0.3b	5.7 ± 0.2a	5.5 ± 0.3a
Totnolobtb	13.9 ± 0.3b	10.3 ± 0.6a	16.3 ± 0.5c	12.3 ± 0.5b	12.3 ± 0.5b
Antposlobrat	0.92 ± 0.04a	1.05 ± 0.05ab	1.13 ± 0.05ab	1.16 ± 0.06b	1.26 ± 0.06b
Anterior deck tubercles					
Anttbden[5]	68.4 ± 2.9a	82.8 ± 3.0ab	81.1 ± 5.9ab	89.8 ± 2.9b	94.7 ± 2.2b
Mnanttbar	1.86 ± 0.05b	1.79 ± 0.05b	1.95 ± 0.14b	1.42 ± 0.05a	1.68 ± 0.05ab
Mnanttbfm[6]	0.477 ± 0.013c	0.447 ± 0.019c	0.282 ± 0.016a	0.311 ± 0.011ab	0.353 ± 0.010b

[1] For definition of abbreviations, see appendix.
[2] Means followed by same letter do not differ significantly.
[3] All linear measurements in μm.
[4] All area measurements in square μm/100.
[5] Number in an area of 400 square μm.
[6] Formfactor = 4 × pi × area/perimeter^2.

Table 2. Additional attributes[1] of eggs of the five species of *An. quadrimaculatus*. Numbers of measurements (n) derived as indicated in superscripts. All area measurements in square μm.

Attribute	Mean (± SE)[2] for species				
	A	B	C1	C2	D
Ventral plastron cells[3]	n = 18	n = 18	n = 18	n = 18	n = 15
Celarvnplas	196.5 ± 6.1ab	181.3 ± 13.2a	286.9 ± 10.9d	245.9 ± 11.6c	234.8 ± 7.6bc
Noporvnplas	40.9 ± 2.1a	44.7 ± 2.5a	48.2 ± 2.4ab	43.6 ± 2.9a	55.9 ± 2.7b
Porarvnplas	1.11 ± 0.09b	1.18 ± 0.11b	0.86 ± 0.05ab	0.75 ± 0.04a	1.15 ± 0.14b
Porarpcnvnplas	22.3 ± 1.5b	28.4 ± 1.2c	14.2 ± 0.6a	13.3 ± 0.9a	25.2 ± 1.6bc
Dorsal plastron cells[3]					
Celardoplas	350.2 ± 11.4ab	358.8 ± 7.5ab	378.3 ± 10.8b	334.6 ± 11.2a	319.9 ± 8.2a
Nopordoplas	46.7 ± 3.6a	58.4 ± 2.8a	106.9 ± 3.3c	91.1 ± 3.5b	53.7 ± 2.4a
Porardoplas	3.72 ± 0.48c	2.83 ± 0.20bc	0.95 ± 0.05a	0.94 ± 0.05a	2.38 ± 0.13b
Porarpcndoplas	42.9 ± 1.3bc	43.7 ± 1.1c	26.4 ± 0.8a	25.3 ± 1.0a	38.9 ± 1.1b
Lobed tubercles[4]	n = 30	n = 30	n = 30	n = 30	n = 25
Antlobtbar	42.0 ± 1.7ab	39.2 ± 1.1a	46.9 ± 0.9b	45.0 ± 1.1b	37.9 ± 1.4a
Antnolobes	7.7 ± 0.2b	7.3 ± 0.3ab	8.1 ± 0.2b	7.4 ± 0.2ab	6.4 ± 0.3a
Micropyle[5]	n = 12	n = 12	n = 12	n = 12	n = 10
Totarmic	656.1 ± 35.3b	461.4 ± 16.1a	650.5 ± 20.3b	539.3 ± 14.9a	515.7 ± 12.9a
Colarmic	391.4 ± 26.4b	286.7 ± 8.8a	391.4 ± 15.3b	330.9 ± 9.9ab	298.1 ± 11.2a
Dskarmic	264.7 ± 11.6c	174.7 ± 10.6a	259.1 ± 10.6bc	208.3 ± 11.1a	217.6 ± 7.7ab
Dskarpcn	40.6 ± 1.1a	37.6 ± 1.4a	39.8 ± 1.3a	38.5 ± 1.5a	42.3 ± 1.4a
Nosect	7.3 ± 0.2a	6.9 ± 0.2a	7.8 ± 0.3ab	7.5 ± 0.2ab	8.2 ± 0.2b

[1] For definition of abbreviations, see appendix.
[2] Means followed by same letter do not differ significantly.
[3] Three cells measured from one egg of each fmeale.
[4] Five tubercles measured from one egg of each female.
[5] One micropyle measured from each of two eggs of each female.

Fig. 1. *Anopheles quadrimaculatus* species A. A, Entire egg, ventral (upper) view, anterior end at top; B, entire egg, lateral view, ventral surface at right, anterior end at top. Scale = 100 μm.

ble 2). To abbreviate the attribute descriptions for tabulation, an acronym designed to be comprehensible in itself was formed for each. Consistent rules of abbreviation were followed: thus, "vn," "do," "ant," "pos," and "rat" are ventral, dorsal, anterior, posterior, and ratio, respectively, with other meanings obvious from the full definitions listed alphabetically in the appendix.

The terminology is that of Harbach and Knight (1980) and, for a few structures, Hinton (1968). The term "outer chorionic cell field" (or "cell field") is defined by Linley (1989).

Fig. 2. *Anopheles quadrimaculatus* species A. A, Outer chorionic tubercles, middle of anterior deck; B, tubercles, middle deck; C, tubercles, posterior deck; D, detail, tubercles on anterior deck; E, detail, plastron of ventral surface; F, lateral surface, dorsal margin of float; G, chorionic cells (plastron), middle of dorsal surface; H, cell detail, middle of dorsal surface. Scale = 20 μm (E, F, G), = 10 μm (A, B, C, H), = 5 μm (D).

RESULTS

Egg of *Anopheles quadrimaculatus* Species A

Size: As in Table 1. *Color*: Black. *Overall appearance*: Boat-shaped in both ventral (Fig. 1A) and dorsal views, anterior end blunt, posterior more pointed. Ventral surface concave, dorsal surface strongly curved, float relatively short and wide in dorso-ventral plane (Fig. 1B).

Dorsal (lower) and lateral surfaces: All surfaces invested uniformly (Fig. 1B) with regularly shaped hexagonal or pentagonal outer chorionic cells (Fig. 2G), each longer (mean 28.0 ± 0.6 μm, n = 18) than wide (mean 16.4 ± 0.4 μm, n = 18). Cell area as in Table 2 and lateral cells contiguous with those of similar structure on ventral surface (see below). In detail, interior (cell field) of each dorsal cell consists of a meshwork supported on very short pillars (the "plastron," Hinton (1968)) perforated by relatively large pores; some of these often fused to create larger, irregular gaps or elongated openings (Fig. 2G,H). Number of pores, their individual areas, and total area as a proportion of cell area given in Table 2. Outer chorionic reticulum bounding each cell consists of a rather indistinct palisade of widely spaced tubercles, these sometimes round or more often elongated along edge of cell and usually joined by a thin parapet (Fig. 2H). Floats fairly short but deep (Fig. 1B); length in proportion to egg length and number of ribs as in Table 1. On dorsal side of float, ribs tending to divide into 2 ridges some distance from dorsal margin, which is irregular and perforated (Fig. 2F).

Ventral (upper) surface: Deck continuous, narrows in mid-line near center of floats (Fig. 1A), degree of narrowing somewhat variable (Fig. 4). Frill continuous, shallow along narrowed portion of deck, deeper at anterior and posterior ends (Fig. 1B). Margins of outer chorionic cells not visible, large tubercles uniformly distributed over entire deck (Fig. 1A), structurally similar in anterior, middle, and posterior deck regions (Fig. 2A–C). Tubercles somewhat smaller in area (not significantly so) in middle region (Table 3), but with significantly higher form factor (defined in Table 1), indicating shape of middle tubercles more closely approximates round. Sides of each tubercle with alternating deep furrows and ridges, the latter sometimes branched (Fig. 2D), tops more or less rounded, often with irregular depressions (Fig. 2D).

Table 3. Mean areas and form factors of tubercles on anterior, middle, and posterior deck regions of eggs of *An. quadrimaculatus* species A.

	Mean (± SE)[1]	
Deck region	Area (sq. μm)	Form factor[2]
Anterior	2.04 ± 0.09a	0.42 ± 0.01a
Middle	1.88 ± 0.08a	0.59 ± 0.02b
Posterior	2.04 ± 0.08a	0.41 ± 0.02a

[1] Means followed by same letter do not differ significantly.
[2] (4 × pi × area)/perimeter^2.

Plastron type cells on ventral surface confined to a narrow strip just ventral to and sometimes contiguous with floats on each side (Fig. 1A), but more often separated from floats by a narrow strip of deck except at anterior and posterior ends (Fig. 4). Detailed structure of ventral plastron cells similar to those on dorsal surface (Fig. 2E). Cell boundaries occasionally difficult to distinguish, but very distinct in most eggs (Fig. 4).

Numbers of lobed tubercles at anterior and posterior ends of deck (also total number) as in Table 1, posterior number significantly greater ($P < 0.05$, t-test). Area and number of lobes in anterior group as in Table 2. Lobed tubercles occasionally round, but more often oval (Fig. 3B,C) and at both ends surrounded by a patch of tubercles that are larger than those on remainder of deck (Figs. 1A; 3A,D). Lobes clearly separated, often swollen at ends (Fig. 3C), outer tubercle walls ornamented with fine ridges.

Anterior end, micropyle: Anterior end prow-like but rounded, collar of micropyle almost touching lower edge of frill (Fig. 3A,B). Quantitative attributes of micropylar apparatus as in Table 2. Outer margin of collar sometimes tending to be hexagonal, but often very irregular (Fig. 3B,F), width variable (Fig. 3F), surface smooth. Inner margin regularly ex-

Fig. 3. *Anopheles quadrimaculatus* species A. A, Anterior end, ventral (upper) surface; B, anterior end, end-on view; C, detail, anterior lobed tubercles; D, posterior end, ventral (upper) surface; E, posterior end, end-on view; F, detail, micropylar apparatus. Scale = 50 μm (A, B, D, E), = 20 μm (C, F).

Fig. 4. Eggs of *An. quadrimaculatus* species (labeled at left) A and B, ventral view; one egg from each of the six females studied (numbered at bottom). Scale = 100 μm.

cavated to form sectors, the apex of each with a thin ridge ("micropylar ray") extending radially toward orifice (Fig. 3F). Disk surface fairly smooth, orifice diameter 1.34 ± 0.05 μm (n = 7), surrounded by a low mound (Fig. 3F).

Posterior end: Distinctly sharper than anterior end (Fig. 3D). Structure of dorsal plastron cells consistent with remainder of dorsal surface, except that cell boundaries difficult to distinguish at very end of egg (Fig. 3E).

Simple, Visual Comparison of Species

There were some obvious visible differences between species. Species A and B eggs (Fig. 4) in almost all cases were distinguishable from species C1, C2 (Fig. 5), and D (Fig. 6) by the extent of ventral area occupied by plastron. Overall, this difference was by far the most easily observable. In species A and B, plastron occupied an average of less than 10% of the ventral area (Table 1) and almost invariably was confined to two strips adjacent to the floats (Fig. 4). It was present as a single, larger area (quite different in appearance) representing between 17 and 24% of the surface (Table 1) in the other three species (Figs. 5, 6). There were occasional inconsistencies within species. Of the 18 species A eggs, all were typical (two separated strips), but in one species B female the strips were unusually wide (Fig. 4, species B, egg 4) and in two other eggs of this female the strips were fused to create an appearance resembling the other species. All the C1 females produced typical eggs (Fig. 5), but although all the eggs of five of the C2 females conformed to this pattern, all three eggs of female 6 (Fig. 5) had two separated strips. Among species D females, all were typical (Fig. 6) except female 4, which had two eggs of the usual type (Fig. 6), one of these with a deep cleft extending anteriorly from the posterior deck, but the third egg had separated but wide strips. With respect to overall shape, species A and B eggs gave the impression of being longer and more slender in appearance (Fig. 4), but this may have been an illusion created by the longitudinally oriented plastron strips and the consequent absence of transverse lines in the image. There were no significant differences between species in the ratio of egg length to width (Table 1). Another impression, in this case supported by objective tests, was that species A and B, particularly the latter, had floats that were shorter in relation to egg length (Figs. 4–6). When compared (Table 1), float length as a percentage of egg length was significantly lower in species B than in any of the others, while species A was lower (not significantly so) than species C1 and C2 but not lower than species D.

At higher magnification, although the appearance of the anterior deck tubercles seemed initially quite uniform (Fig. 7), further inspection suggested that those of species A and B were more compact and rounder in shape, as borne out by their higher form factors (Table 1), which were significantly greater than those of the other three species. The difference in appearance was quite striking in some instances, especially for species C1, in which the tubercles were much more irregular in outline, with relatively much longer peripheral ridges (Fig. 7). Between species C1, C2, and D, form did not seem to differ in any way easily detectable by eye. Species C1 tubercles, however, seemed generally larger, as confirmed by measurement (Table 1). A point of particular interest was that they were significantly larger than those in the very closely related species C2 (Table 1), even though certain C1 females (female 2, Fig. 7) had small tubercles that were indistinguishable from those in species C2.

In the cells of the ventral plastron (Fig. 8) there were rather obvious visible differences, reflected even more clearly in the dorsal plastron (Fig. 9), in terms of pore size and the related attribute of total pore area as a percentage of cell area (Table 2). Species A and B had larger pores, occupying a proportionately greater area of the cell, than species C1 and C2, especially in comparisons of the dorsal surface (Fig. 9, Table 2). Species D occupied an intermediate position (Table 2), but in appearance it resembled species A and B more than species C1 and C2 (Figs. 8, 9).

Fig. 5. Eggs of *An. quadrimaculatus* species (labeled at left) C1 and C2, ventral view; one egg from each of the six females studied (numbered at bottom). Scale = 100 μm.

Fig. 6. Eggs of *An. quadrimaculatus* species D, ventral view; one egg from each of the five females studied (numbered at bottom). Scale = 100 μm.

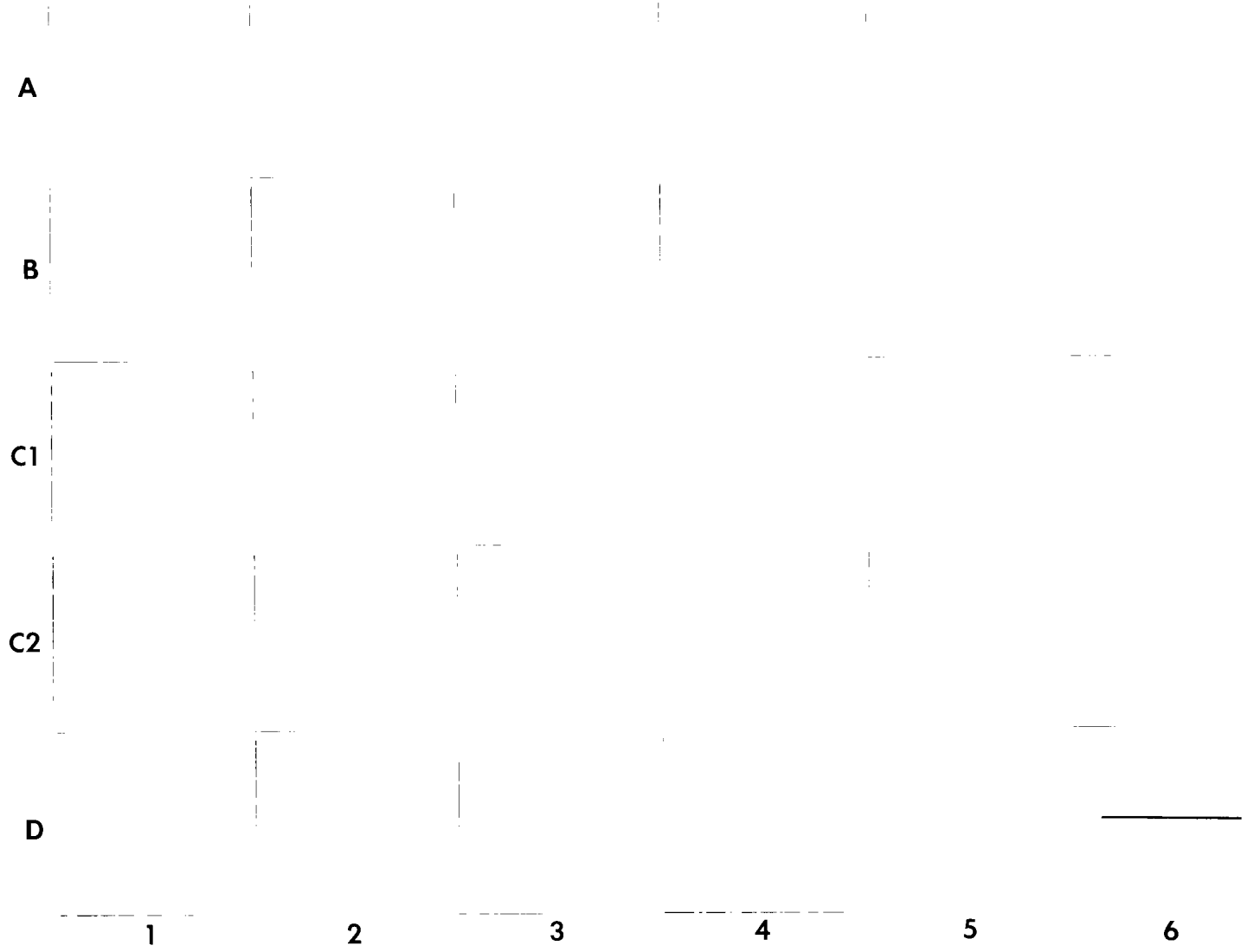

Fig. 7. Tubercles of the middle anterior deck of the five species (labeled at left) of the *An. quadrimaculatus* complex; one egg from each female studied (numbered at bottom). Scale = 10 μm.

Fig. 8. Cells of the ventral (top) plastron of the five species (labeled at left) of the *An. quadrimaculatus* complex; one egg from each female studied (numbered at bottom). Scale = 20 μm.

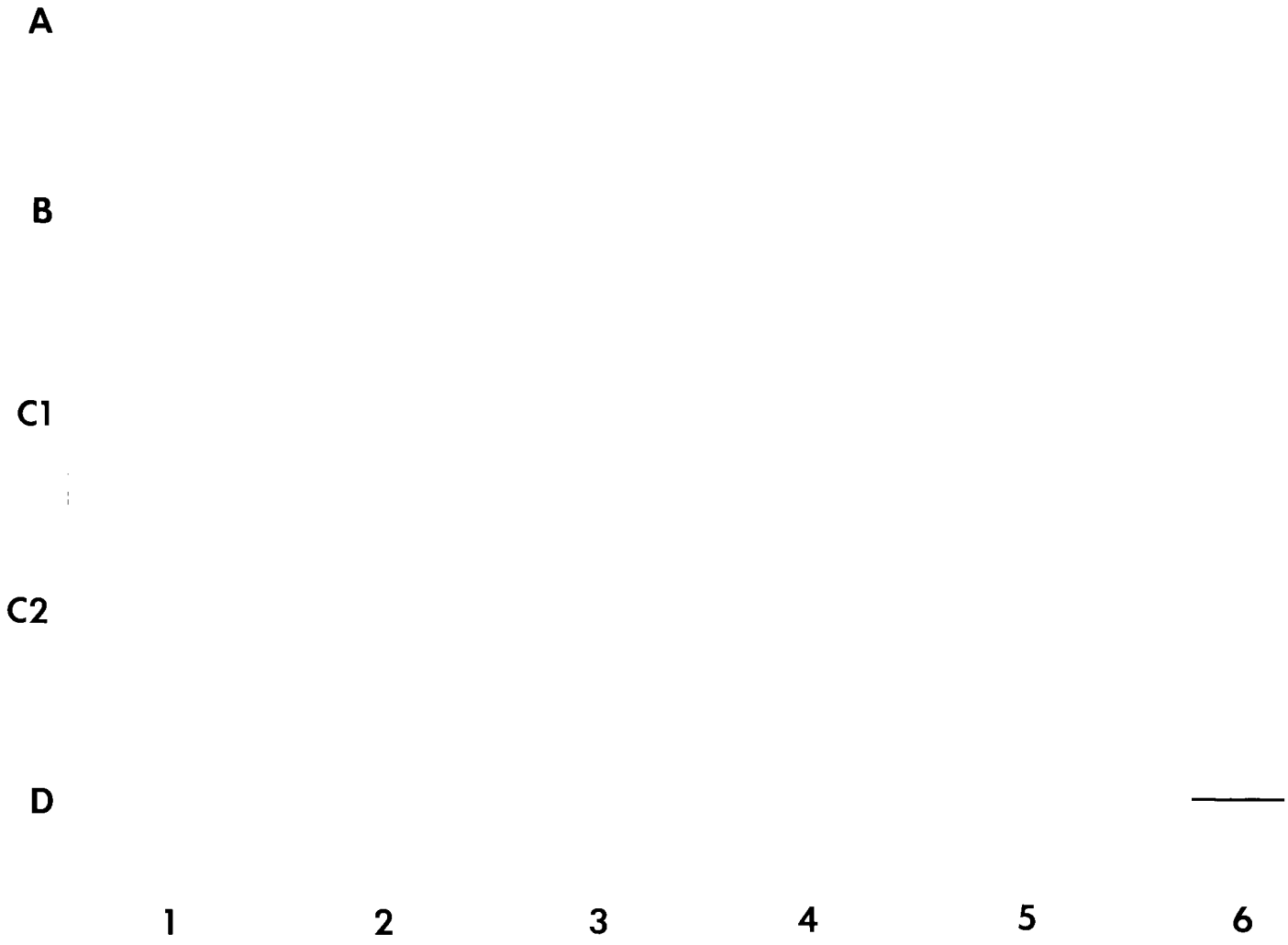

Fig. 9. Cells of the dorsal (lower) plastron of the five species (labeled at left) of the *An. quadrimaculatus* complex; one egg from each female studied (numbered at bottom). Scale = 20 μm.

Table 4. Correlation matrix (lower diagonal form) for 13 attributes of eggs of the five species of *An. quadrimaculatus*.

	Fltpcn	Fltlenprib	Anttbden	Mnanttbar	Mnanttb-fmfac	Totdkpcn
Fltpcn	1.0000					
Fltlenprib	0.3725	1.0000				
Anttbden	0.0945	0.1601	1.0000			
Mnanttbar	−0.0921	−0.0524	−0.7560	1.0000		
Mnanttbfmfac	−0.2352	−0.3245	−0.0261	−0.1511	1.0000	
Totdkpcn	−0.2833	−0.3360	−0.4205	0.2245	0.5612	1.0000
Antdkpcn	−0.2751	−0.3306	−0.3888	0.2193	0.5654	0.9736
Posdkpcn	−0.2731	−0.3189	−0.4290	0.2148	0.5162	0.9608
Vnplaspcn	0.1809	0.2657	0.3088	−0.0757	−0.5326	−0.8597
Dkrat	−0.0234	−0.0085	0.0797	−0.0039	0.1383	0.0306
Posdklenwidrat	−0.1658	−0.1750	−0.2772	0.2316	0.4541	0.5321
Totnolobtb	0.4689	0.2865	−0.2959	0.3055	−0.2727	−0.1133
Antposlobrat	0.0125	0.1712	0.2181	−0.1319	−0.2086	−0.3733

Table 4 continues.

Synoptic Appraisal of Measured Attributes

From the complete tabulations of all the measured attributes (Tables 1, 2), any single interspecific comparison or group of comparisons can be made by examination of the appropriate bloc(s) of data. We therefore touch only briefly on certain features of interest before discussing an appropriate approach to multivariate analysis.

With respect to the floats, those of species A and B, as already mentioned, appeared short relative to the length of the egg and proved to be so on closer examination (Table 1), especially in the case of species B. However, calculation of the length of float occupied by each rib (i.e., rib width) showed that the ribs were narrower in species A and B, with means of 12.4 and 12.3 μm, respectively, as compared with values of 13.2 to 13.6 μm in the other species.

Anterior, posterior, and total deck areas, as well as the respective percentages they constituted of the whole egg area, all conformed to the same pattern among the five species, as evident from significance tests (Table 1). All deck areas were largest (Figs. 4–6) in species A and B, smaller in C1 and C2, and least in D, in which all deck areas formed a significantly smaller percentage of total egg area than in the other four species (Table 1). Percentages of deck area were extremely similar in species C1 and C2, and, when eggs were viewed in groups, the decks did appear somewhat larger in these two species (Fig. 5) than in species D (Fig. 6). The ratios of anterior and posterior deck length to width were, as expected, greatest for species A and B, but in these attributes the values for species D exceeded those for C1 and C2, in agreement with the impression that the decks were relatively narrower in this species (Fig. 6).

In addition to occupying larger areas, the ventral plastron in species C1, C2, and D (Figs. 5, 6) was made up of individual cells that were greater in area (Table 2) compared with the rather elongated cells found in the two narrow plastron strips characteristic of species A and B (Fig. 8). As expected, the larger pores in species A, B, and D resulted in the percentage of cell area occupied by pores in these species being significantly greater than in species C1 and C2 (Table 2). On the dorsal surface, plastron cells were quite uniform in shape, with pore characteristics similar to those on the ventral side, except more easily visible (Fig. 9). There were more pores in the cells of species C1 and C2, and they were significantly smaller than in the other species (Table 2). In terms of individual pore size and percentage of area occupied by pores, species D was intermediate between the two C species and species A and B.

Table 4. *Extended.*

Antdkpcn	Posdkpcn	Vnplaspcn	Dkrat	Posdklen-widrat	Totnolobtb	Antpos-lobrat
1.0000						
0.8720	1.0000					
−0.8530	−0.8064	1.0000				
0.2441	−0.2310	−0.0776	1.0000			
0.5883	0.4258	−0.6345	0.2506	1.0000		
−0.1549	−0.0548	0.2572	−0.1824	−0.2181	1.0000	
−0.3530	−0.3714	0.4059	0.0922	−0.2929	−0.0344	1.0000

Species C1 had a significantly greater total number of lobed tubercles than any other species, while species A, C2, and D were intermediate, and B had significantly fewer (Table 1). In all species except A, there were fewer posterior lobed tubercles than anterior ones, the difference being significant in species C2 and D ($P < 0.05$, <0.01, respectively) and almost significant in species C1 ($P = 0.055$). However, the reverse difference in species A also was significant ($P < 0.05$). This fact, coupled with the low anterior/posterior tubercle ratio also present in species B (Table 1), suggested that individuals of these closely related species tended to have tubercle distributions more posteriorly weighted than species C1, C2, and D. In addition to having the greatest number of lobed tubercles, species C1 also had the largest ones in area (Table 2), and the lobes in them were more numerous than in the other four species. The micropylar apparatus showed significant differences between species in total area, area of collar, and area of disk, all of which were positively correlated (Table 2). Disk area as a percentage of total area, however, did not differ between species. There was some suggestion of a pattern associated with species relatedness in terms of the numbers of sectors on the disk. Species A and B had fewest, C1 and C2 were similar and intermediate, and species D had most (Table 2).

Selection of Characters for Multivariate Analysis

The attributes summarized in Table 2 were not appropriate for inclusion, along with those of Table 1, in any multivariate analysis because their sample sizes were in some cases different and the measurements were not made from the same eggs. Nonetheless, there were 27 characters available in the data contributing to Table 1. Fifteen of these represented direct determinations, either of number (e.g., numbers of lobed tubercles), linear dimension (egg length, width), or area (area of anterior deck), while 12 were "derived" in that they were percentages, ratios, or other values calculated from the data. With respect to characters useful for interspecific differentiation, absolute measurements were deemed to be of relatively less value, as almost all were related to overall egg size. Evidence from previous studies in mosquitoes had shown (Steinwascher 1984) that egg size was partially dependent upon the size of the female, which, in turn, was well known to be influenced by factors operative during larval development (food supply, crowding, temperature). To avoid such influences, we elected to use primarily the derived characters (percentages, ratios), which were more likely to reflect true differences between species. Accordingly, 13 attributes were selected (see

Table 5. Partial tabulation of principal components analysis of correlation matrix (Table 4) of 13 attributes of *An. quadrimaculatus* eggs.

Principal component	Eigenvalue	% of variance	Eigenvector (coefficient)												
			Flt-pcn	Fltlen-prib	Anttb-den	Mnant-tbar	Mnanttb-fmfac	Totdk-pcn	Antdk-pcn	Posdk-pcn	Vnplas-pcn	Dkrat	Posdklen-widrat	Totno-lobtb	Antpos-lobrat
1	5.178	39.83	0.163	0.195	0.208	−0.121	−0.282	−0.419	−0.415	−0.394	0.392	−0.037	−0.299	0.098	0.202
2	2.121	16.31	−0.233	−0.161	0.493	−0.511	0.268	−0.038	0.007	−0.089	−0.056	0.202	0.038	−0.523	0.121
3	1.279	9.84	0.611	0.411	0.281	−0.388	0.161	0.099	0.092	0.103	−0.208	−0.030	0.061	0.266	−0.232
4	1.235	9.50	0.141	0.221	−0.089	0.222	−0.005	−0.065	0.113	−0.277	−0.014	0.787	0.365	−0.009	0.166
5	0.809	6.22	−0.079	0.328	−0.017	−0.041	0.059	0.205	0.160	0.245	−0.053	−0.082	−0.177	0.088	0.839
6	0.692	5.32	0.301	−0.672	−0.035	−0.096	0.298	0.039	0.079	−0.011	0.145	0.252	−0.288	0.388	0.176
7	0.541	4.16	−0.188	0.093	0.106	−0.094	−0.476	0.210	0.276	0.115	−0.055	0.391	−0.595	0.024	−0.254

Table 4), among which only four (float length per rib, anterior tubercle density, mean anterior tubercle area, and total number of lobed tubercles) were direct counts or measurements. Linear or area measurements obviously related to overall size were omitted (e.g., egg length, float length, deck areas).

Principal Components

Unequal scaling of the measurements required initially that the variables each be standardized to zero mean and unit variance, to ensure equal weighting in the analysis. Because the covariance matrix of the standardized variables is the correlation matrix (Table 4), the calculations could be performed on the latter. High levels of correlation between several variables, notably the area percentages of anterior, posterior, and total deck, indicated that the analysis would be successful in describing the variation in terms of considerably fewer components than original attributes.

A partial tabulation of the results (Table 5) shows that the first component accounted for 39.83% of the variation, and the first two accounted for 56.14%. The first seven components explained 91.18% of the variation, so the remaining six were discarded. Considering interpretation of only the first two components in detail, plots were made of the eigenvectors (Fig. 10A) and principal components of the individual eggs (Fig. 10B). Figure 10A indicated that the first component was most positively weighted for ventral plastron percentage (P, Fig. 10A), somewhat less for anterior tubercle density (A), anterior/posterior lobed tubercle ration (O), float length per rib (R), and float length as a percentage of egg length (F). These positive weightings were contrasted with negative values for the three deck areas (D, G, H), which were closely grouped (Fig. 10A), mean anterior tubercle form factor (M), and posterior deck length/width ratio (I). Anterior/posterior deck area ratio (B), total number of lobed tubercles (L), and mean anterior tubercle area (T) had little effect on component 1. Similarly, the second component carried a strong

positive weighting for attribute A and progressively less for M, B, and O, contrasted with moderately negative values for R and F and high negative values for T and L (Fig. 10A). Again, component 2 was little affected by those attributes (D, G, H, I, and P) with coefficients close to zero (Table 5, Fig. 10A).

In terms of individual eggs, species C1, C2, and D clearly separated from species A and B along component 1 (Fig. 10B) as anticipated from these loadings, with the former group at the positive end of the component and the latter at the negative end. Notably, the most heavily weighted attributes, ventral plastron percentage (P) on the positive side and deck area percentages (D, G, H) on the negative, reflected the most obvious visible differences between species C1, C2, and D, and species A and B (Figs. 4–6). Other contrasts indicated by the analysis required high magnification images and were not visible in whole eggs, except to some extent for float length as a percentage of egg length (F), which was positively loaded in component 1 and did appear visibly larger in eggs of species C1, C2, and D (Figs. 4–6). Along component 2, almost all individual eggs of species B and D and most of C2 were positioned on the positive side (Fig. 10B), indicating larger values (Table 1) of the positively weighted attributes (A, M, B, O) and smaller values of characters that were negatively weighted (L, T, F, R). Individual components of species A and particularly C1, on the other hand, were on the negative side, reflecting attribute values (Table 1) that were the reverse of species B, D, and C2. As regards the remaining components (3–7), the eigenvectors can be evaluated similarly (Table 5), but as the percentage of variation explained diminishes, it becomes progressively more difficult to interpret the weightings in terms of attribute differences between species.

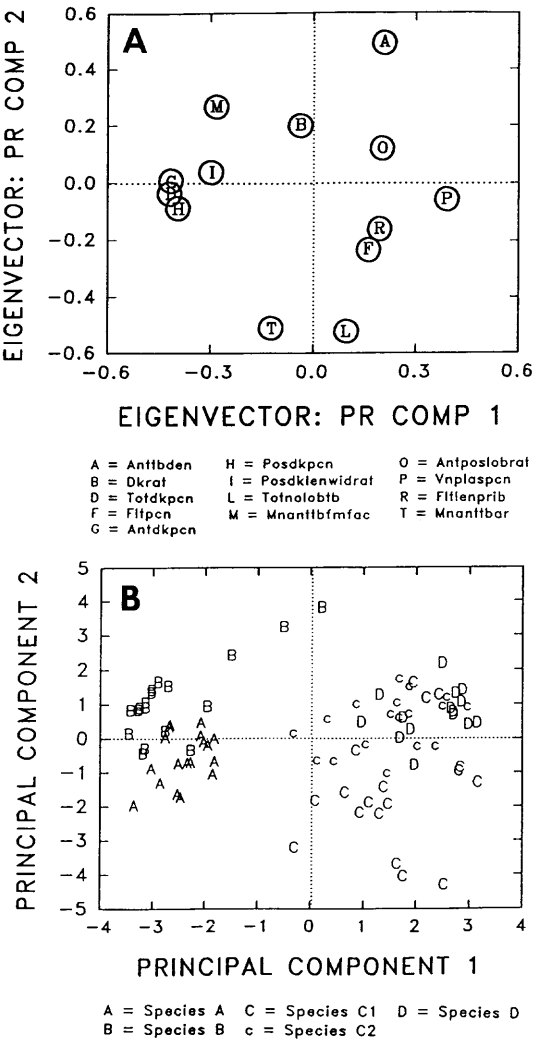

Fig. 10. A, Plot of the eigenvectors of the first two principal components based on 13 attributes of eggs; B, plot of the individual principal components of 87 eggs.

Discriminant Functions

For the same 13 attributes of the eggs, discriminant function analysis was performed on the unstandardized data, as such analyses are unaffected by scaling differences between variables. In discriminant function analysis, linear combinations of the variables are selected so that, in this case, the first function reflected species differences as much as possible, function 2 captured as much as possible of differences not accounted for by function 1, function 3 captured as much as possible of differences not accounted for by functions 1 and 2, and so forth.

The four functions derived (Table 6) were all highly significantly different between species, with function 1 capturing 74.01% of species differences and the second function cap-

Table 6. Summary of discriminant function analysis of 13 attributes of *An. quadrimaculatus* eggs.

Discriminant function	Eigenvalue	Percentage	Chi-square	df	*P*
1	16.525	74.01	444.599	52	<0.00001
2	3.787	16.96	224.099	36	<0.00001
3	1.453	6.51	103.522	22	<0.00001
4	0.563	2.52	34.413	10	<0.0002

turing 16.96%, for a total in the first two functions of 90.97%. Complete tabulation of the coefficients is omitted in the interests of parsimony, but a plot is provided (Fig. 11) of the individual eggs arrayed according to the first two functions, along with the group (species) centroids. There was excellent separation of species A and B from species C1, C2, and D in function 1. In function 2 there was good separation of species A and B, and reasonably good discrimination of species D from species C1. Species C2 was located between species C1 and D, and in this function there was considerable overlap in both directions. However, classification of all 87 eggs on the basis of all four functions yielded 85 (97.7%) correct assignments to species. The two errors were one species C2 egg incorrectly recognized as a species D egg and one species B egg as species A.

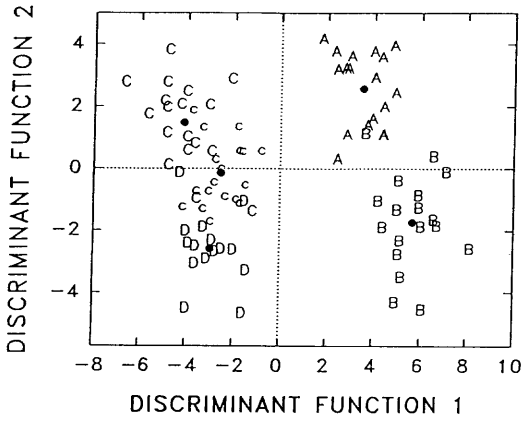

Fig. 11. Plot of the first two individual discriminant functions, based on 13 attributes, of the 87 eggs of species of the *An. quadrimaculatus* complex; group centroids indicated by small filled circles.

DISCUSSION

Although discriminant functions derived from 13 characters will assign eggs to species with considerable accuracy, many of the attributes can be appraised only at magnifications attainable with an electron microscope. Also, the complexities of having simultaneously to evaluate 13 attributes would render species recognition by simple, stereomicroscopic evaluation extremely difficult, even if all the attributes could be seen and measured at this level. On the basis of the eggs examined, species A and B could almost always be separated from species C1, C2, and D by virtue of their proportionately much larger deck areas (conversely smaller ventral plastron areas), coupled with the less evident but nonetheless distinguishably shorter floats (Figs. 4–6). There are, however, occasional inconsistencies that could lead to error, as already pointed out in the simple species comparison above. The only other attributes that might be of value under a light microscope, at least as secondary characters, are associated with the lobed tubercles, which can be counted at low magnification. The to-

Table 7. Numbers, out of 13 attributes, in which each species in the *An. quadrimaculatus* complex was numerically closest (Table 1) to one of the other species.

	Number of attributes closest to species				
Species	A	B	C1	C2	D
A	—	8	2	1	2
B	9	—	1	0	1
C1	1	2	—	7	2
C2	2	1	8	—	8
D	1	2	2	4	—

tal number of these tended to be low in species B, and their numbers in both species A and B tended to be more equally distributed between the anterior and posterior ends (Table 1).

Between species A and B there appeared to be no practicable criteria for distinguishing the two at low magnification. Similarly, species C1 and C2 would be impossible to separate, other than that an unusually high total count (Table 1) of lobed tubercles (>15) would be strongly suggestive of species C1, as only four of the 18 species C2 eggs had as many as this, while 11 of the species C1 eggs had more. The total count of lobed tubercles also could be applied to indicate species C1 rather than D, as only one of the 15 species D eggs examined had a total of 15 tubercles while all the other counts for species D were lower. In other aspects of appearance, species D eggs strongly resembled those of C1 and C2 (Figs. 5, 6), but as indicated in Table 1, both the anterior and posterior deck areas were proportionately smaller in species D and their length/width ratios were greater, indicating both areas to be narrower in relation to length. These differences are to some extent discernible in the whole eggs (Figs. 5, 6) and might be of some use as a tentative index of identity.

As regards phylogenetic relationships, impressions drawn from the eggs generally are in agreement with those drawn from other techniques. Mitochondrial DNA restriction mapping suggested that species C1 and C2 were very closely related, species A and B were related to each other, with the affiliation of species D lying between but on the side of C1 and C2 (Mitchell et al. 1992, AFC and S.E. Mitchell, unpublished data). Isozyme electrophoresis also showed species C1 and C2 as being very closely related and species A and B as related to each other (Narang et al. 1989c, 1990). However, the relationship of species D has not been published. It is obvious, based on outward appearance (Figs. 4–6, and previous discussion), that species A and B are closely associated and the first discriminant function (Fig. 11) clearly separates them from the other three species. The second discriminant function indicates that species C1 and C2 are more akin to one another, and their considerable overlap suggests a closer affinity than between species A and B. The tabulations in Table 7 measure species relatedness based on the relationships of the 13 attributes to each species and bear out conclusions drawn from Fig. 11. Species A is closest to species B and vice versa, species C1 and C2 are nearer each other, and species D is more akin to the C group.

ACKNOWLEDGMENTS

We thank D. Duzak for her particular care in printing the electron micrographs. This paper is Institute of Food and Agricultural Sciences, University of Florida Experiment Station Journal Series No. R-03034.

REFERENCES CITED

Harbach, R.E. and K.L. Knight. 1980. Taxonomists' glossary of mosquito anatomy. Plexus Publishing Inc., Marlton, NJ.

Hinton, H.E. 1968. Observations on the biology and taxonomy of the eggs of *Anopheles* mosquitoes. Bull. Entomol. Res. 57:495–508.

Kaiser, P.E., S.E. Mitchell, G.C. Lanzaro and J.A. Seawright. 1988a. Hybridization of laboratory strains of sibling species A and B of *Anopheles quadrimaculatus*. J. Am. Mosq. Control Assoc. 4:34–38.

Kaiser, P.E., S.K. Narang, J.A. Seawright and D.L. Kline. 1988b. A new member of the *Anopheles quadrimaculatus* complex, species C. J. Am. Mosq. Control Assoc. 4:494–499.

Lanzaro, G.C. 1986. Use of enzyme polymorphism and hybridization crosses to identify sibling species of the mosquito *Anopheles quadrimatulatus* Say. Ph.D. dissertation. University of Florida, Gainesville, FL.

Lanzaro, G.C., S.K. Narang, S.E. Mitchell, P.E. Kaiser and J.A. Seawright. 1988. Hybrid male sterility in crosses between field and laboratory strains of *Anopheles*

quadrimaculatus (Say) (Diptera: Culicidae). J. Med. Entomol. 25:248–255.

Linley, J.R. 1989. Comparative fine structure of the eggs of *Aedes albopictus, Ae. aegypti,* and *Ae. bahamensis* (Diptera: Culicidae). J. Med. Entomol. 26:510–521.

Mitchell, S.E., S.K. Narang, M. Goldenthal, A.F. Cockburn and J.A. Seawright. 1992. Mitochondrial and ribosomal DNA variation among members of the *A. quadrimaculatus* species complex. Genome 35: 939–950.

Narang, S.K. and J.A. Seawright. 1988. Electrophoretic method for recognition of sibling species of anopheline mosquitoes. A practical approach. Proceedings of Symposium, New Technologies for Taxonomic Identification of Arthropods. Florida Entomol. 71:303–311.

Narang, S.K. and J.A. Seawright. 1991. Genetic differentiation among members of species complexes in anopheline mosquitoes (Diptera: Culicidae), pp. 59–96. *In*: R.C. Sobti and G. Obe (eds.), Eukaryotic chromosomes. Narosa Publishing House, New Delhi.

Narang, S.K., P.E. Kaiser and J.A. Seawright. 1989a. Dichotomous electrophoretic key for the identification of sibling species A, B and C of the *Anopheles quadrimaculatus* (Say) complex (Diptera: Culicidae). J. Med. Entomol. 26:94–99.

Narang, S.K., P.E. Kaiser and J.A. Seawright. 1989b. Identification of species D, a new member of the *Anopheles quadrimaculatus* species complex: a biochemical key. J. Am. Mosq. Control Assoc. 5:317–324.

Narang, S.K., J.A. Seawright and P.E. Kaiser. 1990. Evidence for microgeographic genetic subdivision of *Anopheles quadrimaculatus* species C. J. Am. Mosq. Control Assoc. 6:179–187.

Narang, S.K., S.R. Toniolo, J.A. Seawright and P.E. Kaiser. 1989c. Genetic differentiation among sibling species A, B and C of the *Anopheles quadrimaculatus* complex (Diptera: Culicidae). Ann. Entomol. Soc. Am. 82:508–515.

Steinwascher, K. 1984. Egg size variation in *Aedes aegypti*: relationship to body size and other variables. Am. Midl. Nat. 112: 76–84.

APPENDIX

Definitions of abbreviations (acronyms) of measured or calculated attributes of eggs of *An. quadrimaculatus.*

Antdklenwidrat—anterior deck length/width ratio
Antdkpcn—area of anterior deck as % area whole egg
Antlobtbar—mean anterior lobed tubercle area
Antnolobes—anterior lobed tubercle mean number of lobes
Antposlobrat—anterior/posterior lobed tubercles ratio
Anttbden—anterior deck tubercle density
Arantdk—area of anterior deck
Arposdk—area of posterior deck
Artotdk—area of total deck (anterior + posterior)
Arvnplas—area of the ventral plastron
Arwhlegg—area of whole egg (ventral view)
Celardoplas—mean chorionic cell area, dorsal plastron
Celarvnplas—chorionic cell area, ventral plastron
Colarmic—collar area of micropyle
Dkrat—area anterior deck/area posterior deck ratio
Dskarmic—disk area of micropyle
Dskarpcn—disk area as % total apparatus area
Egglen—egg length
Eggwid—egg width (widest point, across floats)
Fltlenprib—mean float length/mean number of ribs
Fltpcn—mean float length as % of egg length
Lenwidrat—length/width ratio
Mnanttbar—mean anterior deck tubercle area
Mnanttbfm—mean anterior deck tubercle form factor

Mnfltlen—mean float length (of the 2 floats)
Mnribs—mean number of ribs (of the 2 floats)
Noantlobtb—number of anterior lobed tubercles
Noplascel—number of ventral plastron chorionic cells
Nopordoplas—mean number of cell pores, dorsal plastron
Noporvnplas—number of cell pores, ventral plastron
Noposlobtb—number of posterior lobed tubercles
Nosect—number of sectors in micropylar disk
Porardoplas—mean individual pore area, dorsal plastron
Porarpcndoplas—total pore area as % cell area, dorsal plastron
Porarpcnvnplas—total pore area as % cell area, ventral plastron
Porarvnplas—mean individual pore area, ventral plastron
Posdklenwidrat—posterior deck length/width ratio
Posdkpcn—area of posterior deck as % area whole egg
Totarmic—total area of micropylar apparatus
Totdkpcn—area of total deck as % area whole egg
Totnolobtb—total number of lobed tubercles
Vnplaspcn—area of ventral plastron as % area whole egg